JOINT EUROPEAN TORUS JET

JET–P(93)07

T.E. Stringer

An Explanation of the L and H Mode Transition Induced by Applied Radial Voltage

An Explanation of the L and H Mode Transition Induced by Applied Radial Voltage

T.E. Stringer

JET-Joint Undertaking, Culham Science Centre, OX14 3DB, Abingdon, UK

Preprint of a paper to be submitted for publication in Nuclear Fusion
February 1993

ABSTRACT

The response of the edge plasma to an applied voltage is analysed. When the anomalous transport is ambipolar, the radial current is determined by neoclassical fluxes. An equation is given for the neoclassical radial current which is valid across the transition between the plateau and the collisional viscous regimes. The current at first increases with the applied field, E, and then decreases due either to the resonant velocity band being pushed to the tail of the ion velocity distribution or to a decrease in viscous damping. Thus the same current can be driven by two different electric fields, E_1 or E_2. This allows an equilibrium field profile, where E changes abruptly from E_1 to E_2 at some intermediate radius, while maintaining current continuity. It is shown unambiguously that a continuous electric field profile becomes unstable when the applied voltage exceeds a critical value, the instability being driven by negative incremental resistivity. The profile then bifurcates to one with discontinuous electric field.

Qualitatively, the predicted behaviour agrees well with that observed in tokamaks where an H-mode has been induced using a biased electrode. Quantitative comparisons are made with TEXTOR results, and the predictions found to be in qualitative agreement with measurement. The implications for spontaneous L-H transitions are discussed.

1. INTRODUCTION

The improved confinement regime, known as the H-mode, was first observed to occur spontaneously in large divertor tokamaks [1 - 3] when the neutral beam power exceeds a threshold value. It was later found that a similar plasma behaviour can be produced in Ohmic-heated limiter plasmas by applying sufficient voltage to a probe some centimeters inside the plasma [4 - 6]. In both conditions the onset of the H-mode is characterised by a sharp reduction in the H_α (or D_α) radiation, indicating a large reduction in recycling, and the sudden appearance of a strong radial electric field in the outer centimeter or so of the plasma. In the probe-triggered H-mode the potential profile between probe and limiter changes abruptly from a smooth variation to one where most of the potential change is concentrated in a narrow edge region. In both cases the strong radial electric field seems to occur simultaneously with the improved confinement, before the pressure profile has changed significantly [7]. This suggests that the change in field is the cause, rather than the effect, of the improvement.

Several possible explanations have been proposed for the spontaneous H-mode transition [e.g. 8 - 10]. Because it is difficult to evaluate the hot ion orbit loss accurately and to measure the profiles of electric field and other parameters, it has not been possible to make a definitive comparison between theory and experiment. By contrast, the triggering of an H-mode by applying a voltage can be done in a controlled way, and the lower edge temperature allows the electric field and other profiles to be measured using Langmuir probes. The similarities with the spontaneous L to H-mode transition suggest that the two processes have much in common. This paper sets out to make a detailed prediction of the plasma response to an applied voltage, and to compare this with measurement. Comparison will be made with recent results from TEXTOR [5], because they form the most complete set of published data. The related problem of the effect of the electric field on the particle and energy confinement will not be discussed.

The behaviour of the radial electric field, E_r, produced by an applied voltage is attributed in Ref. [5] to a decrease in perpendicular conductivity towards the plasma edge, due mainly to decreasing density. In the equation $j_r = \sigma_r E_r$, rj_r is constant between probe and limiter, so E_r varies inversely as the conductivity σ_r.

It is not obvious how this can explain the sudden transition from smooth electric field profile to one concentrated at the edge, especially as the change in field is thought to precede the change in density profile.

This paper proposes a different explanation. As the radial electric field increases, the neoclassical radial current at first increases linearly, and then passes through a maximum before decreasing at higher fields. Beyond the maximum the incremental resistivity is negative, which makes the electric field unstable to the growth of a space charge perturbation. This instability evolves into a second equilibrium profile, in which the current is everywhere continuous but the electric field has a discontinuity. The bifurcation from a smooth radial variation in electric field to a discontinuous one, when the voltage exceeds a threshold, is qualitatively similar to the observed behavior in probe-triggered H-modes.

Section 2 discusses the neoclassical radial current over the transition from the plateau to the viscous collisional regimes. The response of a uniform plasma to an applied voltage is analysed in Section 3, where the instability in the electric field profile, above a threshold voltage, is discussed. The evolution of this instability is traced to a second equilibrium, where there is an abrupt discontinuity in the radial electric field at some intermediate radius. The analogous behaviour in the realistic case of an edge plasma with strong radial variation in pressure is studied in Section 4. Section 5 makes a detailed comparison of the predicted behavior with the TEXTOR measurements. The relevance of this analysis to the spontaneous L to H transition is discussed briefly in Section 6, and the conclusions are set out in Section 7. In several places where the detailed analysis is not essential for the general understanding, it is relegated to an appendix. These appendices include a summary of the derivation of the neoclassical particle fluxes over the transition between plateau and viscous collisional regimes, the stability of potential profiles and, when unstable, their evolution to a new equilibrium.

2. RADIAL CURRENT IN A NEOCLASSICAL PLASMA

The current in the plateau regime will be described first, followed by its generalisation to include collisional effects. The original neoclassical analysis of

Galeev and Sagdeev [12] for the plateau and banana regimes led to expressions for the particle flux of the form

$$\Gamma_j^N = -nD_j \left[\frac{n'}{n} + \gamma_j \frac{T_j'}{T_j} - \frac{e_j}{T_j}\left(E_r - B_\theta U_{j\|}\right) \right] \exp\left[-\left(E_r / B_\theta v_{tj}\right)^2 \right] \qquad (1)$$

where j = i or e denotes ions or electrons. In the plateau regime, $\gamma_j = 3/2$ and

$$D_j = \frac{\pi^{1/2}}{2} \epsilon^2 \frac{\rho_j}{r} \frac{T_j}{e_j B_\theta} \qquad (2)$$

where $\epsilon = r/R$ is the inverse aspect ratio, $\rho_j = \sqrt{2T_j m_j} / eB$ the Larmor radius, B_θ the poloidal magnetic field, $v_{tj} = (2T_j/m_j)^{1/2}$ is the thermal velocity, $U_{j\|}$ the mean velocity along the magnetic field, and the other notation is standard.

For a plasma without internal electrode, where neoclassical transport is the only source or loss mechanism, or if the other loss mechanisms are ambipolar, quasi-neutrality requires $\Gamma_i^N = \Gamma_e^N$. Since $D_e = 0\ (m_e/m_i)^{1/2} D_i$, this requires the first bracket in the ion flux to cancel to this same order, giving the ambipolar electric field

$$E_a = \frac{T_i}{e}\left(\frac{n'}{n} + \gamma_i \frac{T_i'}{T_i} \right) + B_\theta U_{i\|} \qquad (3)$$

where a dash denotes differentiation with aspect to the radius.

It has frequently been stated that neoclassical transport is automatically ambipolar, enabling the electric field to be eliminated from Eq. (1). The argument for this is based on the flux-surface-averaged momentum balance and so, as discussed in Ref. [11], is valid only when there is no momentum source other than neoclassical processes. In the present problem, anomalous momentum loss must occur, as otherwise the $j_r B_\theta$ force would produce acceleration in the toroidal direction. The radial electric field is now determined by the voltage applied to the probe, and Eq. (1) determines the neoclassical current produced by this E_r. Even when the overall diffusion is dominated by

electrostatic turbulence, the radial current still equals the neoclassical current, because the fluxes produced by electrostatic fluctuations are ambipolar.

Previous discussions of the L to H-mode transition have frequently used a momentum balance argument [8]. The first velocity moment of the kinetic equation gives a momentum equation, in which kinetic effects such as Landau damping are included in a generalised pressure tensor. Although the two approaches are equivalent, evaluation of the particle flux by solving the kinetic equations is physically clearer and, in this particular problem, the results are easier to apply than those in terms of viscous stress and poloidal damping.

The electron contribution to the current may be neglected. The radial current in response to an applied electric field can then be written as

$$j_r = \frac{Kp_i}{r}(x - x_a)\exp\left(-x^2\right) \tag{4}$$

where $x = E_r/v_{ti}B_\theta$, $x_a = E_a/v_{ti}B_\theta$, $K = \pi^{1/2}\epsilon^2/B$, and $p_i = nT_i$. The origin of the exponential factor is as follows. Neoclassical transport is predominantly due to particles whose poloidal velocity is small, because their magnetic drift is radially unidirectional for longer times. Since $rd\theta/dt = (v_{||}B_\theta - E_r)/B$, the resonant velocity band is centered on $v_{||} = E_r/B_\theta$. When this exceeds the thermal velocity, the number of resonant particles falls off strongly. The maximum and minimum in j_r occur at E_m where

$$E_m = \frac{1}{2}\left[\pm\sqrt{2v_{ti}^2 B_\theta^2 + E_a^2} - E_a\right] \tag{5}$$

Usually $E_a/v_{ti}B_\theta \sim T_i/(eL_n v_{ti}B_\theta) = \rho_{i\theta}/L_n << 1$ where $\rho_{i\theta}$ is the ion Larmor radius in the poloidal magnetic field, and L_n is the density scale length. Then $E_m \approx \pm v_{ti}B_\theta/\sqrt{2}$. The variation in current with E_r is illustrated by curve (a) in Fig. 1.

We now consider the limits of validity of the plateau analysis. In a complete treatment, the neoclassical transport includes a contribution from resonant (or trapped particles) and one from the collisional diffusion of the bulk plasma. In the more usual condition, where $E_r = o\,[(dp/dr)/ne]$, the transition between the

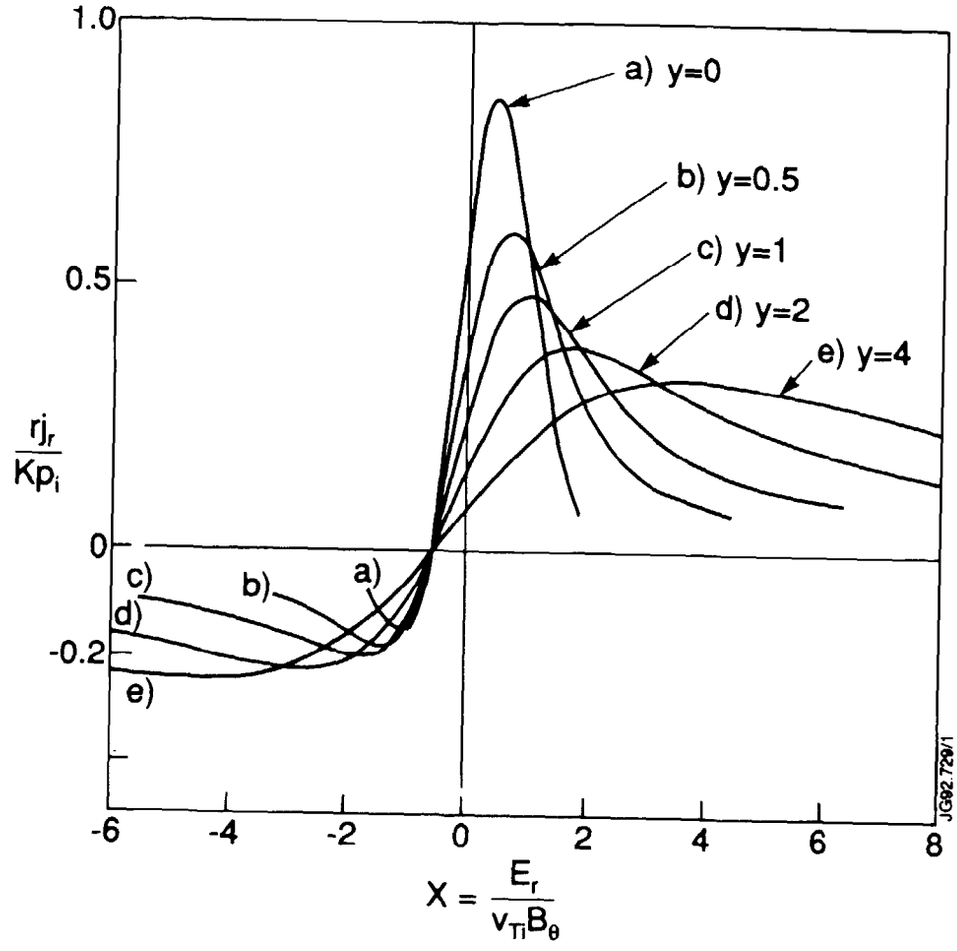

Fig. 1 The variation of the normalised neoclassical radial current with the normalised radial electric field for x_a = - 0.6 and different collisionalities, $y = qR/\lambda_{mfp}$.

collisional regime and the plateau regime where resonant particle effects are dominant, occurs when λ_{mfp}, the mean free path, equals qR. For larger electric fields, $E_r > B\theta v_{ti}$, because the contribution of the resonant particles is exponentially reduced, the collisional contribution is dominant up to mean free paths longer than qR.

The transition between the plateau and collisional regimes was studied by Connor and Stringer [13], starting from the kinetic equation with a BGK collision operator. A short summary of this analysis is given in Appendix A. It neglected the velocity dependence of the collision operator but, since this paper is aimed at physical understanding rather than exact numerical agreement, this velocity dependence is not essential. The complete expression for the ion flux in Eq. (A7), which includes the effect of the poloidal electric field E_θ, is long. In the following analysis, only the first term in this equation will be used. The other terms, which result from E_θ, from higher order $v_\parallel$ moments arising from the curvature drift, and from imposing conservation of particles and momentum during collisions, make a comparable contribution, but do not change the asymptotic behavior of the ion current. (The effect of $E\theta$ was neglected by Galeev and Sagdeev when deriving Eq. (1), and in most other analyses.) The radial current can then be written in a form analogous to Eq. (4).

$$j_r = \frac{Kp_i}{r}(x - x_a)\frac{1}{\pi^{1/2}}\,\mathrm{Im}[Z(x,y)] + j^{ps} \qquad (6)$$

where $Z(x,y) = \frac{\perp}{\pi}\!\!\!/_2 \int_{-\infty}^{\infty} \frac{e^{-t^2}}{t-z}\,dt = e^{-z^2}\left[i\pi^{1/2} - 2\int_0^z e^{t^2}\,dt\right]$,

$$z = x + iy, \qquad y = \frac{r\nu_{ii}}{v_{ti}\Theta} \equiv \frac{qR}{\lambda_{mfp}}, \qquad \Theta = \frac{B_\theta}{B}$$

and ν_{ii} is the ion-ion collision frequency. In the following analysis λ_{mfp} is defined as v_{ti}/ν_{ii}. Because $v_{ti} = [2T_i/m_i]^{1/2}$, this is $2^{1/2}$ times the usual mean free path. Im [Z(x,y)] is tabulated by Fried & Conté [15]. It equals $\pi^{1/2}$ u(x,y) where u(x,y) has been tabulated by Fedeeva & Terentev [16]. j^{PS}, which is proportional to the electron-ion collision frequency, is a generalisation of the

Pfirsch-Schlüter radial flux, valid for arbitrary electric field. It is numerically small in all the applications of present interest and will be neglected.

It is obvious that when $\nu_{ii} = 0$, Eq. (6) agrees with Eq. (4) for the plateau regime. If, on the other hand, we take the large y limit [15] of Eq. (6) we obtain

$$j_r = \frac{Kp_i}{r\pi^{1/2}}(x - x_a)\frac{y}{x^2+y^2} \tag{7}$$

In the collisional limit where $r\nu_{ii} >> E_r/B$ this becomes

$$j_r = \frac{\epsilon^2}{\sqrt{2}}\frac{ne\ \rho_i}{Br^2}\frac{v_{ti}}{\nu_{ii}}(E_r - E_a) \tag{8}$$

This is e times the ion diffusion rate when parallel ion viscosity is dominant and the poloidal electric field is neglected [17]. Eq. (6) thus describes the smooth transition from the plateau to the viscous regimes. When $E_r > v_{ti}\ B_\theta$, the collisionality at which this transition occurs depends strongly on the radial electric field, as illustrated in Fig. 3 of Ref. [13].

Fig. 1 shows how

$$(x - x_a)\frac{1}{\pi^{1/2}}\,\mathrm{Im}\left[Z(x,y)\right] = \frac{r}{Kp_i}\,j_r \tag{9}$$

varies with $x = E_r/v_{ti}\ B_\theta$ for several values of $y = qR/\lambda_{mfp}$. The value of $x_a = E_a/v_{ti}\ B_\theta$ has been kept constant at -0.6. Fig. 1 illustrates the competition between Landau and viscous damping, mentioned at the beginning of this section. When $0 < qR/\lambda_{mfp} < 1$, the dissipation at moderate electric fields ($x \le 0.5$) is dominated by Landau damping, producing a plateau-like particle flux, while at larger electric fields collisional viscous damping may become dominant. Increasing collisionality reduces the Landau damping, but increases viscous damping when $E_r > r\nu_{ii}B$ (see Eq. (7)). These two trends move the maximum of j_r to higher E_r so that, when $qR/\lambda_{mfp} >> 1$, Eq. (5) is replaced by

$$x_m \approx x_a \pm \left[x_a^2 + y^2\right]^{1/2}$$

3. RESPONSE OF A UNIFORM PLASMA TO AN APPLIED VOLTAGE

As may be seen from Eq. (6), the local neoclassical radial conductivity depends on local parameters. The radial variation in parameters will be taken into account in Section 4, where the response of a model edge plasma is considered. There the basic simplicity of the bifurcation process becomes rather obscured by the effects of inhomogenity. The bifurcation may be understood more easily when the radial variation in plasma parameters is ignored.

The boundary condition is $\int E_r \, dr = V$, where V is the voltage applied to the probe and the integration is between the probe and limiter radii. To be specific, we consider the case where V is positive and hence E_r is outwards, though the analysis is equally valid when V is negative. The conditions are that j_r is related to E_r by Eq. (6), and that in a steady state, rj_r must be constant to avoid build-up of space charge (in this section the r factor will be ignored).

The most obvious solution has a uniform electric field, $E_r = V/s$, where s is the separation between the probe and limiter radii, and a current found by

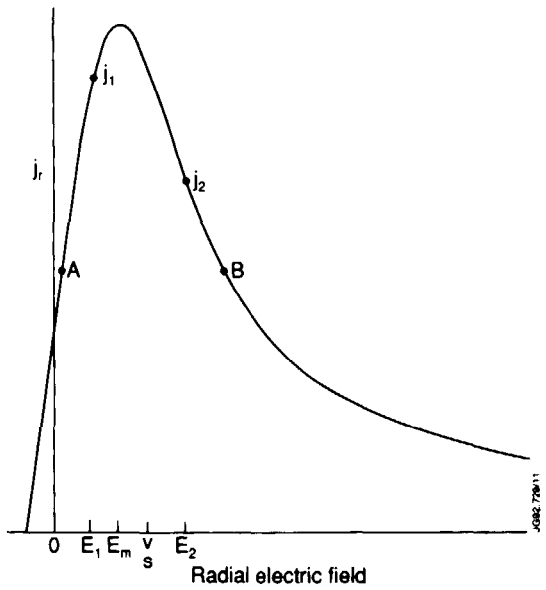

Fig. 2: Local current vs. electric field

substituting for E_r in Eq. (6). It was previously assumed that, as V is increased, the plasma current follows the variation shown in Fig. 1. for the appropriate

value of qR/λ_{mfp}. Thus, j_r at first increases linearly, reaches a maximum, and subsequently decreases, as illustrated in Fig. 2. That this does not happen in practice can be seen by considering the stability of such an electric field to a localised space charge perturbation when $V > sE_m$, where $E_m(y)$ is the electric field at which the current reaches its maximum.

Suppose a small positive space charge occurs around some intermediate radius $r = a-d$. This produces a small increase in E_r as we cross the space charge, as illustrated in Fig. 3. Since $\int E_r\, dr$ must be unchanged, E_r is decreased slightly

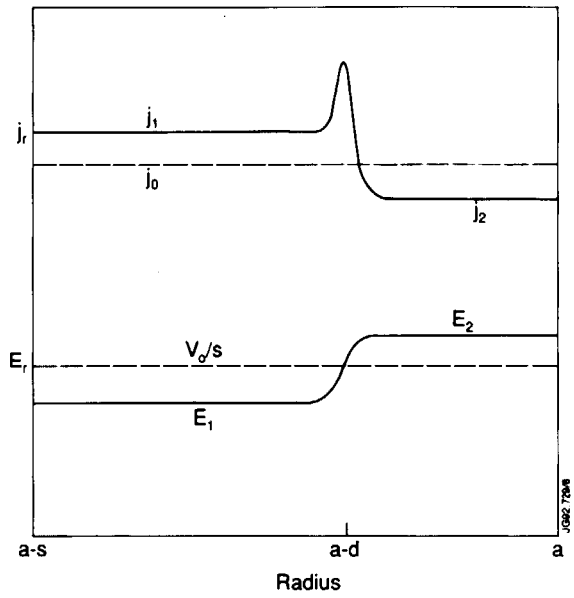

Fig. 3: Electric field and current profiles resulting from a localised space charge around r = a-d.

over $r < a-d$, and increased over $r > a-d$. This causes j_r to increase over $r < a-d$, and to decrease over $r > a-d$. This produces an increase in the space charge near $r = a-d$, and hence an exponential growth in the electric field jump. The instability is driven by the negative incremental resistance when $E > E_m$. When $E < E_m$ a similar argument shows, of course, that the constant E_r profile is stable. (If the momentum equation were used instead of Eq. (1), rotational instability occurs when $v_\theta > E_m/B$ because the poloidal flow damping decreases as the magnitude of this flow increases).

The evolution of an unstable E_r profile is examined in Appendix B. Only a brief description will be given here. The radial ranges $a-s < r < a-d-\delta$ and $a-d+\delta < r < a$, will be denoted by subscripts 1 and 2 respectively, where δ is the

half-width of the space charge distribution. At some value of the space charge, E_1 is pushed below E_m in Fig. 2. The space charge continues to build up because j_1 is still greater than j_2, but now j_1 decreases with time. Because the slope of the current response is steeper when $E < E_m$ than when $E > E_m$, j_1 decreases more rapidly than j_2, and eventually they reach equality, as illustrated by points A and B on Fig. 2. The build-up of space charge then ceases. As discussed in Appendix B, the space charge distribution, which has been becoming narrower during the build-up, may continue to narrow until it reaches a lower limit imposed by ion Larmor radius effects. The transition from E_1 to E_2 is then so abrupt that it can be regarded as discontinuous. The discontinuous electric field profile satisfies the equilibrium conditions. Thus $\int E\, dr = V$ has been satisfied during the evolution, and now j(r) is everywhere constant.

When $V > sE_m$, the constant E_r equilibrium is unstable to an initial space charge perturbation at any radius between the probe and limiter radii. Consistent with this, discontinuous equilibria can exist with discontinuity anywhere within this range. The stability of this second equilibrium is not as obvious as for the constant electric field profile. It is analysed in Appendix C where it is found, not surprisingly, that it is stable to a change in the field discontinuity when $E > E_m$, and unstable when $E < E_m$. However, when $E > E_m$ the discontinuous field profile is found to be unstable to the growth of a charge perturbation located between the discontinuity and the limiter. While such a perturbation evolves into a new electric field discontinuity, the original discontinuity at r = a-d dies away. Thus it would seem that the only completely stable profile has a discontinuity close to the limiter. In practice the foregoing analysis is probably not valid within some distance b from the limiter, where neutrals, impurities, and ion orbit loss current are important. In this case the stable electric field profile when $V > sE_m$ has a discontinuity at r = a-b.

Thus if the voltage applied to the probe is increased from zero, the predicted response is as follows: So long as $V < sE_m$ the electric field is constant over the radial zone between the probe and limiter. When V exceeds sE_m we expect a bifurcation, as the electric field suddenly changes to a discontinuous equilibrium, where E_r is constant over each of two regions, changing discontinuously between them. The discontinuity is expected to be located one poloidal Larmor radius or more from the limiter radius. While $V < sE_m$ the radial current increases steadily

with voltage. At the instant of bifurcation the current drops abruptly to a lower value, and then decreases with further increase in voltage.

4. RESPONSE OF AN INHOMOGENOUS PLASMA

We now include in the model the variation in plasma parameters across the edge region, and examine the analogues of the continuous and discontinuous electric field profiles found in the homogenous plasma. Fig. 4 illustrates the variation of rj_r/Kp_i with x for specified values of y and x_a, as given by Eq. (9) (i.e. one of

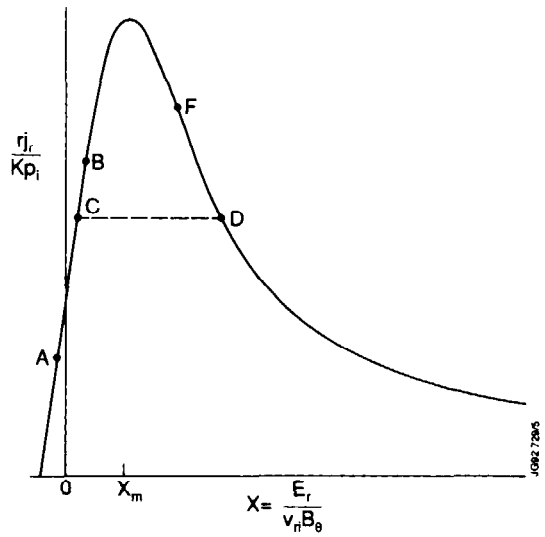

Fig. 4 Typical variation of normalised current with electric field

the curves in Fig. 1). rj_r must be constant across the annulus between the probe and limiter radii. If rj_r is specified, and $p_i(r)$ is known, then rj_r/Kp_i is a known function of r. The corresponding values of x, which can be read from this figure or calculated from Eq. (9), then give E_r as a function of r. Integrating E_r over r gives the applied voltage. If the voltage is specified a priori, the value of rj_r can be adjusted until $\int dr\, E_r$ takes the specified value.

In the usual condition where $p_i(r)$ decreases monotonically between the probe and limiter radii, rj_r/Kp_i increases with radius, reaching its maximum value rj_r/Kp_a at the limiter. The variation of $K = \pi^{1/2}\, \epsilon^2 /B$ is relatively weak

compared with p_i, and will not be explicitly considered. Let us start with a low applied voltage. The resulting current is also relatively low, and the variation in rj_r/Kp_i could correspond to the section AB on Fig. 4. (A corresponds to the probe radius and B to the limiter radius). As the voltage is increased, the range in x must move to higher values, i.e. point B moves further up the curve. At some critical voltage V_c the upper limit of the x range reaches x_m, i.e. B reaches the current maximum. For higher voltages a continuous electric field equilibrium is impossible, because the point B cannot move on to the descending portion of the response curve, since rj_r/Kp_i must increase monotonically between probe and limiter. Hence we must change to a discontinuous field profile.

A discontinuous field equilibrium is illustrated by the sequence ACDF on Fig. 4. As radius increases from r = a-s, the representative point moves up the positive slope with increasing rj_r/Kp_i. At some radius, r = a-d, E_r jumps across to the decreasing section. There is no change in current in this jump. As p_i decreases further with increasing radius, the point moves up the negative slope section, reaching F when r = a. The total voltage is larger than is possible with a continuous equilibrium, because of the contribution from the high field side. As voltage increases, the current decreases because the field in the outer region is pushed further out on the tail of Fig. 4.

As an example, we consider a simple linear pressure profile over the edge region, $p_i = p_a\,[1 + g(a-r)/s]$. Typical values for these parameters during the probe experiment on TEXTOR [5] are $p_a = 3.10^{13}$ eVcm^{-3}, g = 6, s = 6 cm. The electron temperature varied only weakly over the edge plasma in these experiments [5] and so T_i will be taken as constant. For this example the collisionality is taken as $qR/\lambda_{mfp} = 1$. Fig. 5 shows, for g = s, where s is the probe-limiter spacing in cm, how the normalised current, rj_r/Kp_a varies with the position of the discontinuity for specified values of the normalised voltage, $\alpha = V/v_{ti}\,B_\theta\,s$. For each value of α there is now a limited range of d/s within which the equilibrium conditions can be satisfied. The maximum value of rj_r/Kp_i for these parameters is 0.35. At each α, the maximum value of d/s corresponds to rj_r/Kp_i reaching this value at r = a, i.e. to point E in Fig. 4 reaching the current maximum. The critical value of α, above which a continuous field profile is impossible, is 0.22.

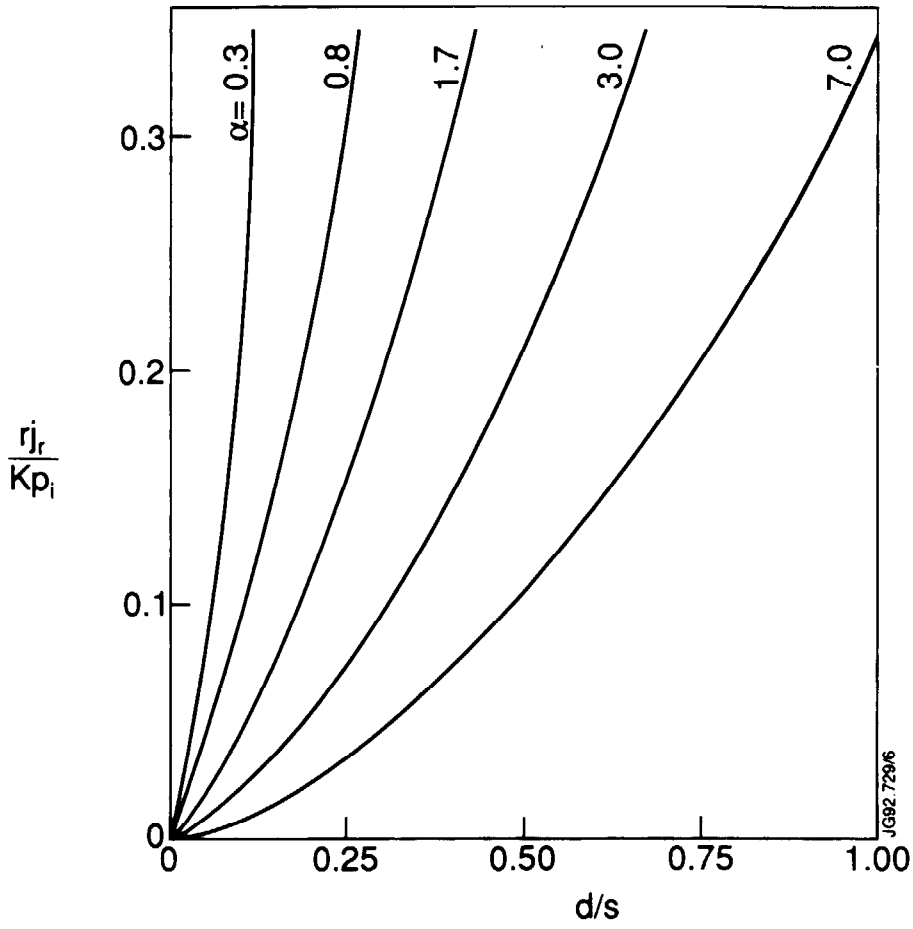

Fig. 5: Variation of the normalised current with position of the discontinuity, for the normalised voltages specified ($\alpha = V/v_{ti}B_\theta$ *s)*

Thus, in an inhomogenous plasma, bifurcation to a discontinuous electric field profile occurs when the applied voltage exceeds a critical value, which in the above example is given by $\alpha = 0.22$. When the voltage is slightly larger than critical, the discontinuity must occur close to the limiter radius, the width of the allowed range increasing with the applied voltage.

5. COMPARISON WITH TEXTOR RESULTS

In TEXTOR a voltage was applied to a carbon electrode situated between 6 cm and 4.5 cm inside the limiter radius [5]. The floating potential and plasma parameters were measured by a double Langmuir probe, whose radial resolution is 1 mm. Fig. 6, reproduced from Ref. 5, shows the radial variation in the floating potential over 1.5 cm inside the limiter radius at 46 cm. The voltage of the probe relative to the limiter, V_E, is shown on each curve. When $|V_E| < 450$ volts the floating potential increased (or decreased) fairly uniformly between the electrode

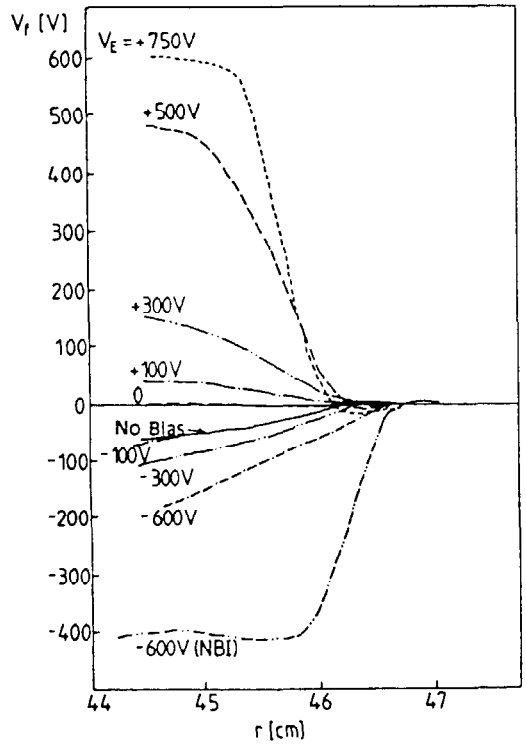

Fig. 6: Radial profile of the floating potential in TEXTOR for different voltage applied to an electrode located between r = 40 cm and 41.5 cm

and limiter. An abrupt change in profile shape occurs when V_E exceeds about 450 volts. Nearly all the voltage drop now occurs within about 1 cm from the limiter, where the total electric field can reach 1 kV/cm. For the remaining 4 - 5 cm to the electrode radius, the electric field is an order of magnitude less.

Simultaneously with the change in profile shape, the plasma showed most of the characteristics of an L to H transition. There was a marked reduction in the D_α radiation, and the particle confinement time increased by factors of 2 to 4 (although the energy confinement time increased by only 15% to 30%). The profile change was accompanied by an abrupt reduction in the current between probe and limiter [5] as shown in Fig. 7.

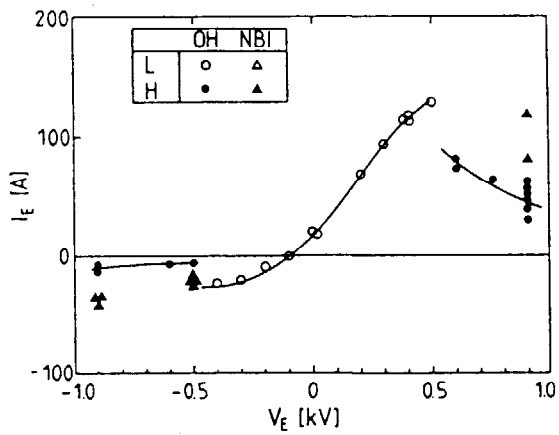

Fig. 7: Variation of electrode current I_E with electrode voltage in TEXTOR for different conditions identified in the inset [5].

The abrupt change in the potential profile when the applied voltage exceeds a threshold, shown in Fig. 6, agrees very well qualitatively with the bifurcation predicted in Sections 3 and 4. We now make some quantitative comparisons. Typical parameters for the deuterium edge plasma during the experiments in TEXTOR are $n_e = 2.10^{12}$ cm^{-3}, $T_e = 40$eV, B = 2.35 T, $\epsilon = 0.26$, q = 7. This makes $\nu_{ii} = 1{\cdot}2.10^4$/sec and $qR/\lambda_{mfp} = 2.6$. To allow for a low impurity content, this will be increased to $qR/\lambda_{mfp} = 4$. We first estimate the threshold voltage. At threshold rj_r/Kp_i reaches its maximum value of 0.35 at r = a. Its value at other radii is then 0.35 p(a)/p(r). The values of x at different radii can be taken from the appropriate curve in Fig. 1, and E_r then integrated over radius. Using TEXTOR parameters, and again approximating p(r) by p(a)[1+ a-r], where a-r is in cm., leads to a threshold voltage of 93 V. (In this calculation, x_a varied from

0.8 at r = a to 0.4 at r = a-d.) We now compare this with the uniform plasma model of Sec. 3, where the current maximum occurs at $x_m = 3.8$ (see Fig. 1). This corresponds to an electric field $E_r = 3.8.10^{-2}\, v_{ti}\, B_\theta$ (where v_{ti} is in m/sec and B_θ in Tesla), giving a threshold voltage of about 1 kV.

To see the reason for this large difference in thresholds, consider the non-uniform plasma at an applied voltage just below threshold. Then in Fig. 4 point B, which corresponds to r = a, is close to the current maximum at $x = x_m$. One centimeter into the plasma, $p_i(r) = 2\, p_i(a)$, and hence rj/Kp_i is one half its maximum value. The corresponding value of x, and hence E_r, is much less than E_m, as may be seen from Fig. 1. This is illustrated in Fig. 8, which shows the radial variation in E_r in (a) a uniform and (b) a non-uniform plasma, in both cases just below threshold. In the non-uniform plasma the electric field reaches the critical value at one point only, and everywhere else is well below critical. Obviously $\int E_r\, dr$ is much less than for a uniform plasma, where E_r is everywhere at the critical value.

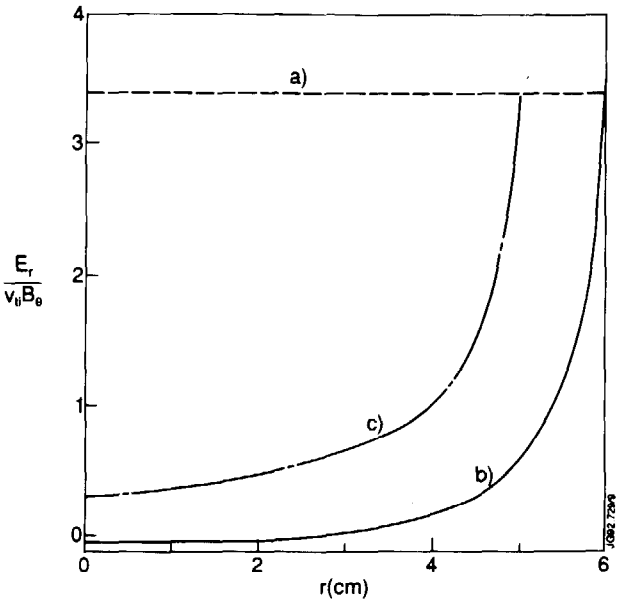

Fig. 8: Radial variation in electric field for (a) uniform plasma, (b) non-uniform plasma, (c) non-uniform plasma with ion orbit loss

The predicted rapid radial variation in E_r near the limiter radius is not seen experimentally in Fig. 6. This casts doubt on the assumption that rj_r is constant there. Variation in rj_r could result from fast ion orbit loss. Those ions which become trapped within about one poloidal Larmor radius, $\rho_{i\theta}$, from the limiter radius have orbits which penetrate into the limiter shadow. The loss of such fast ions as they strike the limiter gives rise to an ion current. The condition that rj_r must be constant refers to the total current, so any ion orbit loss current must be balanced by a reduction in the neoclassical current, referred to in future as j_r^N.

Since it is difficult to evaluate the ion orbit loss current accurately, the convenient assumption will be made that rj_r^N is constant over $a\text{-}d < r < a\text{-}\rho_{i\theta}$, while rj_r^N/Kp_i is constant within a distance $\rho_{i\theta}$ from the limiter radius. In the TEXTOR edge plasma, $\rho_{i\theta}$ is about 1 cm, so this implies that the ion orbit loss current increases from zero at 1 cm into the plasma to about half the total current at r = a. Curve c in Fig. 8 shows the radial variation in E_r just below threshold resulting from this assumption. Integrating this between electrode and limiter radii gives the threshold voltage for bifurcation to be 400 V. This is close to the experimental value, of about 450 V.

The predicted electric field profile after bifurcation depends on the position of the discontinuity which is not determined by the foregoing analysis. Assigning the experimental value $d \approx 1$ cm, the predicted jump in E_r when $V_E = 500$ V is from 100 V/cm to 330 V/cm, while when $V_E = 750$ V the predicted jump is from 37 V/cm to 670 V/cm. These fields are all within 50% of the experimental values which, in view of the assumptions, is perhaps as good as can be expected.

Fig. 9 shows the variation in the predicted electrode current with the applied voltage, for positive voltages. The calculated curve is similar in shape to the

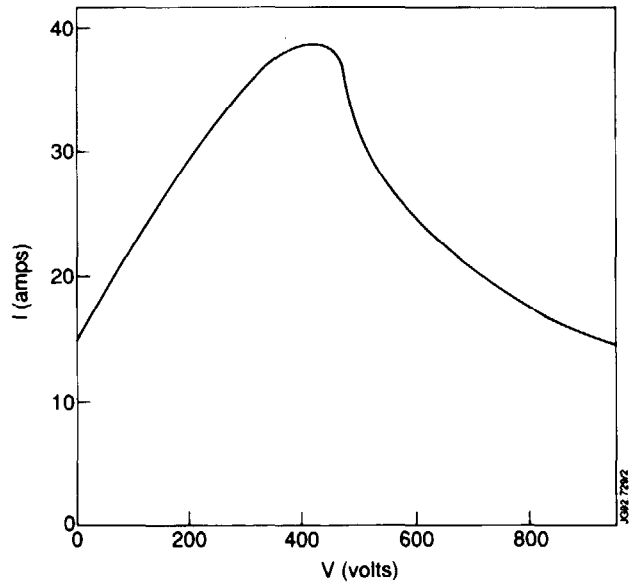

Fig. 9: Variation in predicted plasma current with applied voltage., y = 4, x_a = 0.4 to 0.8.

experimental current dependence in Fig. 7, but its magnitude is only about one third of the measured current. This discrepancy might be due to the neglect of some terms in going from Eq. (A7) to Eq. (6). The neglect of these terms does not

change qualitatively the ion current dependence, but could introduce a discrepancy factor of order unity.

We now consider the plasma response to a negative applied voltage. From Eq. (4), the only dependence of the plasma conductivity on the sign of the electric field is through the $(x-x_a)$ factor. For the density and temperature profiles measured in TEXTOR, the ambipolar electric field, Eq. (3), is expected to vary between -30V/am at r = a and -20V/cm at the probe radius. Thus the effective conductivity is less when E_r is negative than when it is positive, as shown in Fig. 1.

The electrode properties can be more important in determining the current. As pointed out by Weynants et al. [5], when the applied voltage in TEXTOR is negative, the current to the electrode must consist of ions collected from the surrounding plasma, since the electrode is not emissive. This ion absorption is balanced by an inward neoclassical ion flow. After the current reaches the ion saturation current, any further voltage increase produces an ion deficiency around the electrode. The electric field outside this sheath region is that required by Eq. (6) to drive the ion saturation current through the plasma. The remainder of the applied voltage appears as the potential drop across the region of ion deficiency, as illustrated by curve (a) in Fig. 10. The local plasma current required to balance the ion saturation current at the electrode is everywhere below the maximum neoclassical current, and hence there is no bifurcation. In TEXTOR steady H-modes were not observed in Ohmic plasmas with negative applied voltage. However, a negative H-mode could occur when neutral beam injection (NBI) was added, and a pure Ohmic H-mode persisted after NBI was switched off [5].

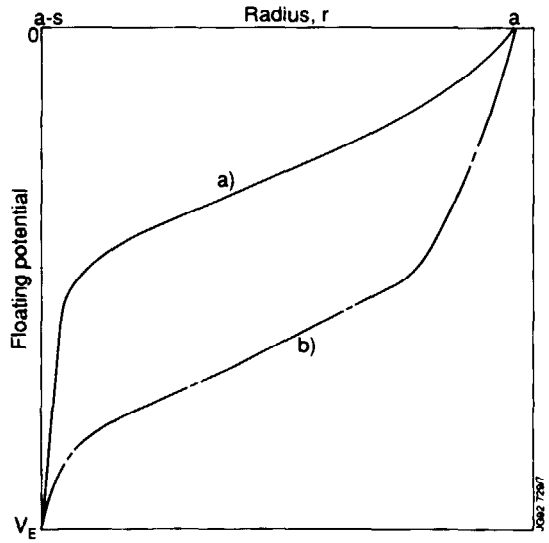

Fig. 10: Potential Profiles (a) without NBI and (b) with NBI

The explanation could be as follows. NBI increases the fast ion orbit loss current in the outer edge. Thus the inward ion neoclassical current there must increase to balance this current as well as supplying the current to the electrode. Let us suppose that this combined current exceeds the maximum neoclassical current. Since the inward neoclassical current cannot balance the orbit loss, an ion deficiency builds up leading to a rapid increase in the inward electric field near the plasma edge, with a consequent reduction in the potential increase across the electrode sheath. The former effect reduces the ion orbit loss current, due for example to orbit shrinking [18], while the latter reduces the current flow to the electrode. The negative charge build up ceases when the sum of these two currents falls below the maximum that can be balanced by the neoclassical current. During this transitional phase E_r becomes large over the outer edge plasma, and consequently when the new equilibrium is established $E_r > E_m$, i.e. the equilibrium is a discontinuous one. Curve (b) in Fig. 10 illustrates such a potential profile.

Finally we consider what happens when NBI is switched off. The inward neoclassical ion flux suddenly drops to that required to supply the electrode current. But since $E > E_m$ in the outer edge plasma, decreasing current requires an increase in the electric field there (see, for example, Fig. 4). There is a balancing decrease in E_r over the inner edge plasma, and the electrode current may drop below its saturation value. The electric field, however, is still discontinuous, and the plasma should retain the characteristics of an H-mode. The above sequence of equilibria agrees qualitatively with the behaviour of the potential profiles and electrode current at negative voltage in Fig. 6 and 7.

6. RELEVANCE TO SPONTANEOUS L TO H TRANSITIONS

The strong inward radial electric fields observed in spontaneous H-modes are larger [7] than the ambipolar value in Eq. (3), and so the neoclassical ion flux, given by Eq. (6), is inwards. This implies the presence of a non-ambipolar ion loss mechanism, the neoclassical current being required to prevent the build-up of negative space charge. Shaing and co-workers [8] and Itoh and Itoh [9] propose the loss of trapped ions whose orbits enter the divertor or strike a limiter. This gives rise to an outward ion current, which starts from zero at about one banana width inside the plasma boundary and increases towards the boundary. Shaing's mechanism will now be outlined and, where it is not consistent with the foregoing analysis, modifications will be proposed, and some extensions made.

Shaing and co-workers [8] derived their equilibrium by balancing the torque exerted by the escaping trapped ions against the viscous damping of the poloidal rotation. Because we find the equivalent description in terms of ambipolar currents easier to apply and more physically transparent, we re-express Shaing et al's. argument in these terms, using the foregoing analytic results.

The argument is best illustrated by Fig. 11 which is a modification of one given by Shaing and Crume [8]. The dashed lines show the current carried out of the plasma by those trapped ions whose orbits enter the divertor or limiter shadow, using Shaing and Crume's [8] formula with $\alpha = 0.25$. The solid lines show the neoclassical ion current, as given by Eq. (6), with its sign changed. The plasma collisionality parameter, qR/λ_{mfp}, decreases from figures (a) to (b) to (c). The ambipolar electric field, defined by $j^N(E_r) + j^L(E_r) = 0$, where $j^L(E_r)$ is the orbit loss current, is given by the intersection of the curves. Fig. 11(a) represents an L-mode plasma. Only one ambipolar field is possible, which is less then $v_{ti}\, B_\theta$. In Fig. 11(b) there are three possible ambipolar fields, but the middle one can be shown to be unstable, using an argument like that in Appendix C. As the plasma evolves from condition (a) to condition (b), the electric field may be expected to continue at the lowest ambipolar value of $|E_r|$. When the plasma moves into condition (c) this intersection disappears near the boundary and the electric field is forced to jump to the further ambipolar value. This discontinuous jump in E_r is identified with the observed sudden appearance of a strong electric field and transition to H-mode confinement. Unlike the plasma with applied voltage, considered in Section 3, the equilibrium with $E_r > E_m$, i.e. on the decreasing part of the j vs x curve, is now stable against a space charge perturbation.

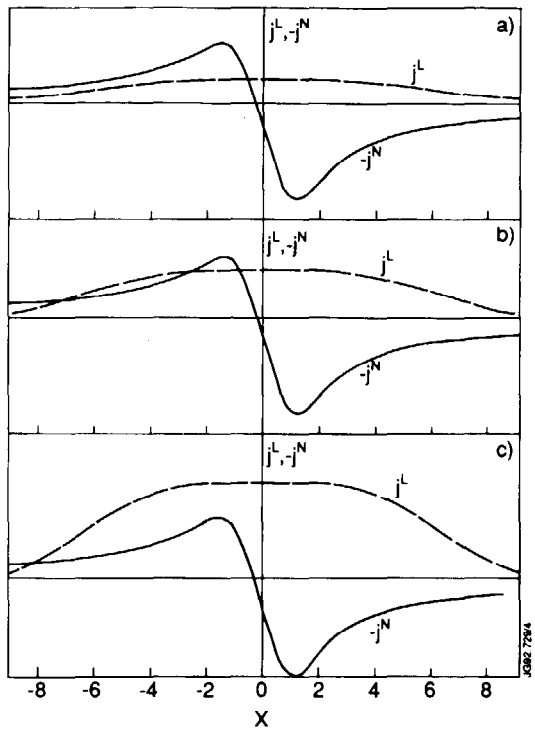

Fig. 11:Variation in the neoclassical and ion orbit loss currents with $x = E_r/V_{ti}B_\theta$. qR/λ_{mfp} decreases from figs. (a) to (c).

Shaing et al. [8] attribute the transition between Fig. 11 (a), (b) and (c) to a reduction in the neoclassical ion current, due to a decrease in collisional viscosity

with increasing temperature. In conditions where H-modes occur experimentally, the edge plasma is in the plateau or collisional viscous regimes. As may be seen from Fig. 1, the neoclassical radial ion current does not decrease there with decreasing collisionality. In fact, the peak current increases weakly, while the extremum occurs at lower values of $|E_r|$. A more plausible explanation for the evolution from case (a) to case (c) is the increase in density of trapped ions as the edge temperature increases, leading to an increase in the ion orbit loss current.

The above discussion ignores the radial variation across the edge region. Fig. 11 can also be used to illustrate the changing conditions as the radius approaches the separatrix. The ion orbit loss current curve increases in magnitude from zero at distances from the boundary greater than an orbit width, reaching its maximum at the boundary. Over the same radial range, the neoclassical current curve decreases in magnitude with the pressure. Fig. 12 shows how the ambipolar electric fields vary with radius over the edge region. Fig. 12(a) corresponds to an L-mode. On the left of the sketch, the plasma is in the condition illustrated in Fig. 11(a). As the ion orbit loss current increases with radius it enters condition 11(b). Since there is no mechanism for generating a jump in electric field, it stays on the lowest branch. Fig. 12(b) corresponds to an edge temperature above the threshold for the L-H transition. Close to the boundary the only ambipolar electric field lies on the upper branch, necessitating a jump from the lower to the upper branch. The only qualitative discrepancy between the above sequence and the experimental behavior is that the jump in electric field is expected to occur from A to B in Fig. 12(b). At the onset of the H-mode, the width of the high field region then starts from zero and increases steadily with increasing temperature. Experimentally, however, the high field region has a finite width at the onset of the H-mode, and this width

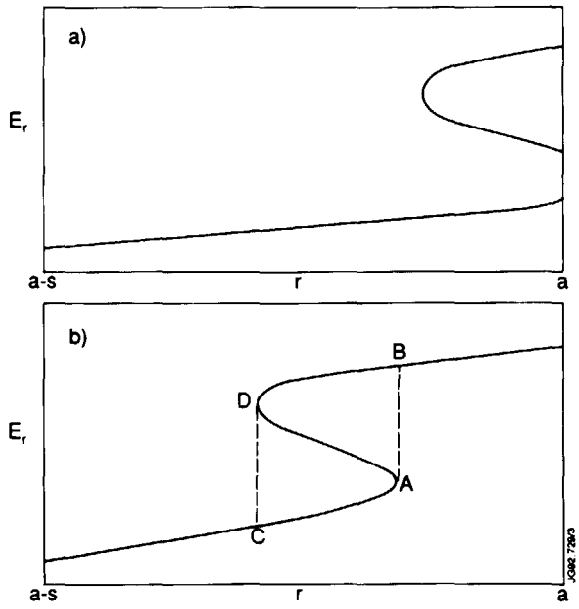

Fig. 12: Variation of ambipolar electric field with radius for (a) an L-mode, (b) an H-mode

does not change much as the parameters exceed threshold. The equilibrium conditions are satisfied by a jump anywhere between CD and AB. A jump near CD would remove the above discrepancy but, within the present model, there is no reason to expect this jump anywhere but at AB. Possibly some other physics, such as impurity effects, prevents a jump in E_r too close to the boundary.

7. CONCLUSION

1. The processes leading to an L-H bifurcation in the edge plasma may be described either in terms of current balance, where the ion current is derived directly from the kinetic equation, or in terms of momentum balance based on the velocity moment of this equation. The former approach is preferred here. This allows the use of earlier results for the smooth transition in the neoclassical ion current as collisionality changes from the plateau to the collisional regimes. A large radial electric field reduces Landau damping as the resonant velocity is pushed on to the Maxwellian tail. The transition from plateau to ion viscous neoclassical behavior then occurs at a collisionality lower than the usual criterion $\lambda_{mfp} = qR$.

2. Detailed predictions are made for the electric field and plasma current produced by applying a voltage to an internal electrode. A bifurcation is predicted when the applied voltage exceeds a well-defined threshold. The origin of this bifurcation is easily understood when the radial variation in plasma parameters is ignored. The neoclassical ion current reaches a maximum at a specific radial electric field E_m, and decreases for higher fields. The negative incremental resistivity leads to an instability in which a localized charge perturbation grows exponentially. It continues to grow and becomes more sharply localized, until a second equilibrium is reached. In this equilibrium there is a discontinuity in the electric field, from E_1 to E_2, at the location of the initial perturbation, such that $j(E_1) = j(E_2)$. Simultaneously there is an abrupt decrease in the current. This behavior agrees qualitatively with what is observed in CCT, [4], TEXTOR [5] and TUMAN 3 [6]. In our model the discontinuity is completely stable only when it is close to the limiter radius, but other effects may limit how close it can occur.

3. To make realistic predictions, the radial parameter variation should be included. For a stationary equilibrium the plasma radial current must be constant across the edge plasma. For a specified applied voltage and pressure profile, this dictates the radial variation in E_r. Now bifurcation first occurs when the electric field at the boundary reaches E_m. For higher applied voltages the only possible equilibrium has an electric field discontinuity.

4. A first estimate of the voltage at which bifurcation should occur in TEXTOR yields a value about one fifth of that observed [5]. Its value is dominated by the variation very close to the plasma boundary. The ion orbit loss current, due to trapped ions which do not return to the plasma because their orbits intersect the limiter or divertor, is likely to be important within one poloidal Larmor radius from the boundary. Since the total ion current must be constant, the neoclassical ion current is reduced as the boundary is approached. Choosing as an example an ion orbit loss current, which at the boundary reaches half the total current, gives the threshold voltage for bifurcation close to that observed. The predicted jump in electric field at the discontinuity is consistent with measurement.

5. The predicted variation in plasma current with applied voltage is similar to that measured in TEXTOR. However, the magnitude of the predicted current is only about one third of the measured value.

6. The above comparisons are with measurements made when the applied voltage is positive. The marked difference in plasma response when the applied voltage is negative arises because the electrode is not emissive. Hence the current which a negative electrode can draw from the plasma is limited by the ion saturation current. The electric field in the plasma is that required to drive a neoclassical current of this magnitude, the remainder of the voltage appearing as a sheath potential at the probe. The electric field in the plasma is everywhere less then E_m, so there is no bifurcation. It was found that an H-mode can be created in TEXTOR by adding NBI to a plasma with negative applied voltage, and that the

H-mode persisted after the NBI is switched off [5]. This behaviour can be explained qualitatively in terms of the foregoing analysis.

7. Although the spontaneous L to H mode transition is not considered in detail, much of the analysis is also applicable to this problem, and the implications are discussed qualitatively. The explanation for bifurcation proposed by Shaing and co-workers [8] is still generally valid, though some modifications are needed. In particular, as the temperature increases, the decrease in the ion neoclassical current seems less important than the increase in the ion orbit loss current. The argument is extended to include the radial variation in these currents. The high electric field region is predicted to be very thin immediately after bifurcation and to increase steadily as the edge temperature rises beyond threshold. This is contrary to the experiment, where the width of the high field region at the H-mode onset is comparable to the poloidal Larmor radius and changes little as the parameters increase beyond threshold.

ACKNOWLEDGEMENT

It is a pleasure to thank D. Ward for many helpful discussions and comments.

REFERENCES

[1] Wagner, F., Becker, G., Behringer, K., Phys. Rev. Lett. 49 (1982) 1408

[2] Burrell, K.H., et al., Plasma Phys. and Controlled Fusion Research, 1988, (IAEA Vienna, 1989) Vol. 1, p. 193

[3] JET Team, Plasma Phys. & Controlled Fusion Research 1990 (IAEA Vienna, 1991) Vol. 1, p. 261

[4] Taylor, R.J., Brown, M.L., Fried, B.D., et al., Phys. Rev. Lett. 63 (1989) 2365

[5] Weynants, R.R.,van Oost, G., et al., Nuc. Fusion 32 (1992) 837

[6] Askinazi, L.G., et al., Nuc. Fusion 32 (1992) 271

[7] Groebner, R.J., Burrell, K.H., Seraydarin, R.P., Phys. Rev. Lett. 64 (1990) 3015

[8] Shaing, K.C., Crume, E.C., Phys. Rev. Lett. 63 (1989) 2369
Shaing, K.C., Crume, E.C., Houlberg, W.A., Phys. Fluids B2 (1990) 1492,
E.C., Shaing, K.C., Phys. Fluids B4 (1992) 290

[9] Itoh, S.I., Itoh, K., Nuc. Fusion 29 (1989) 1031

[10] Hassam, A.B., Antonsen, T.M., Drake, J.F., Liu, C.S., Phys. Rev. Lett., 66 (1991) 309

[11] Stringer, T.E., Nuc. Fusion 32 (1992) 1421

[12] Galeev, A.A., Sagdeev, R.Z., Sov. Phys. JETP 26, (1968) 233

[13] Connor, J.W., Stringer, T.E., Phys. Fluids 14 (1971) 2184

[14] Stringer, T.E., Connor, J.W., Phys. Fluids 14 (1971) 2177

[15] Fried, B.M., Conté, S.D., The Plasma Dispersion Function, Academic Press, New York and London, 1961

[16] Fedeeva, V.N., Terentev, N.M., Tables of Values of the Probability Integral for Coupled Arguments. State Publishing House for Technical Theoretical Literature, Moscow, 1954

[17] Stringer, T.E. Phys. Fluids 13, (1970) 1586.

[18] Hazeltine, R.D., Phys. Fluids B1 (1989) 2031.

[19] Gross, E.P., Krook, M., Phys. Rev. 102 (1956) 593.

[20] Stringer, T.E., Phys. Fluids 13 (1970) 810.

[21] Hinton, F.L., Rosenbluth, M.N., Phys. Fluids 16 (1973) 836.

[22] Stringer, T.E., Phys. Fluids B3 (1991) 981.

APPENDIX A

GENERALISED NEOCLASSICAL ANALYSIS FOR THE PLATEAU AND COLLISIONAL REGIMES

The derivation of Eq. (6) for the neoclassical ion current, valid in both the plateau and collisional viscous regimes, and the effect of poloidal electric field on it, will now be briefly outlined. The analysis starts in Ref. [14] with the drift equation for the guiding centre distribution function $f\left(r,\ \theta,\ v_{\|},\ v_{\perp}^2\right)$ with a BGK collision operator [19],

$$\left(\underline{V}_j \nabla\right) f_j + \frac{\partial f_j}{\partial v_{\|}} \frac{dv_{\|}}{dt} + \frac{\partial f_j}{\partial v_{\perp}^2} \frac{dv_{\perp}^2}{dt} = -\sum_k \nu_{jk} \left\{ f_{1j} - \left[\frac{n_{1j}}{n_o} + \frac{2 q_k v_{\|}}{v_{tj}^2} \right] f_{oj} \right\} \quad \text{(A1)}$$

where $\underline{V}_j$ is the guiding centre velocity, ν_{jk} is the collision frequency of the j^{th} species on the k^{th} species, and $q_k = \int d^3 v f_{1k} v_{\|}$ is the poloidally varying part of the mean parallel velocity of the k^{th} species. Subscript zero denotes the flux-surface-averaged parameter, and subscript 1 denotes the $o(\varepsilon)$ poloidal variation. The collision operator conserves particles and momentum, but not energy. The neglect of temperature perturbation in the collision operator is equivalent to assuming large parallel thermal conductivity. The zero order distribution function is assumed to be locally Maxwellian, and is written in the form.

$$f_{oj}\left(r,\ v_{\|},\ v_{\perp}^2\right) = \frac{1}{\pi v_{tj}^2} \exp\left(-v_{\perp}^2 / v_{tj}^2\right) F_{oj}(r, v_{\|})$$

$$F_{oj} = \left[n_o(r) / \pi^{1/2} v_{tj} \right] \exp\left(-v_{\|}^2 / v_{tj}^2\right).$$

The analysis, although straightforward, becomes very lengthy. To illustrate the method, the first step will now be shown. The zero order particle velocity consists of the electric drift, $v_o = - E_{ro}/B$, and the velocity $v_{\|}$ along the magnetic field. The first order acceleration terms are [20].

$$\frac{dv_{\|}}{dt} = - \frac{1}{m_j v_{\|}} \left(\underline{v}.\nabla\right) \left(e_j \Phi_1 + \mu B\right)$$

$$\frac{1}{v_\perp^2}\frac{dv_\perp^2}{dt} = \frac{1}{B}(\underline{v}.\nabla)B = \frac{(v_o + \Theta v_\parallel)}{R}\sin\theta$$

where $\Theta = B_\theta/B$, $B \approx B_o\,(1 - \varepsilon\cos\theta)$, and $\Phi_1(r,\theta)$ is the poloidal variation in electrostatic potential. The first equation follows from $v_\parallel = \left[\left(\xi - e_j\Phi - \mu B\right)2/m_j\right]^{1/2}$, where ξ is the particle energy and the second from conservation of the magnetic moment, $\mu = m_j v_\perp^2/2B$. Linearising Eq. (A1) in ε gives

$$(v_o + \Theta v_\parallel)\frac{1}{r}\frac{\partial f_{1j}}{\partial\theta} - \left[\frac{\left(v_\parallel^2 + v_\perp^2/2\right)}{\Omega_j R}\sin\theta + \frac{1}{rB}\frac{\partial\Phi_1}{\partial\theta}\right]\frac{\partial f_{oj}}{\partial r}$$

$$+\left[\frac{e_j\Theta}{m_j r}\frac{\partial\Phi_1}{\partial\theta} - \frac{1}{R}\left(\frac{1}{2}v_\perp^2\Theta - v_o v_\parallel\right)\sin\theta\right]\frac{2v_\parallel}{v_{tj}^2}f_{oj} - \frac{(v_o + \Theta v_\parallel)}{R}\sin\theta\,\frac{v_\perp^2}{v_{tj}^2}\,f_{oj}$$

$$= -\sum_k \nu_{jk}\left\{f_{1j} - \left(\frac{n_{1j}}{n_o} + \frac{2q_k v_\parallel}{v_{tj}^2}\right)f_{oj}\right\} \qquad \text{(A2)}$$

Now write $\sin\theta = [\exp(i\theta) - \exp(-i\theta)]/2i$, and f_{1j}, n_{1j}, Φ_1, and q_k in the form $f_{1j} = f_{j+} + f_{j-}$, where f_{j+} and f_{j-} vary as $\exp(i\theta)$ and $\exp(-i\theta)$ respectively. The equation for f_{j+} is

$$\left(v_o - ir\nu_j + \Theta v_\parallel\right)f_{j+} = \frac{\epsilon}{2v_{tj}^2}\left(v_o + U_{nj}\right)\left(v_\perp^2 + 2v_\parallel^2\right)f_{oj}\exp(i\theta)$$

$$+\left(U_{nj} - \Theta v_\parallel\right)\frac{e_j\Phi_1}{T_j}f_{oj} - ir\nu_j\frac{n_{j+}}{n_o}f_{oj} - \frac{2iv_\parallel r}{v_{tj}^2}f_{oj}\sum_k \nu_{jk}\,q_{k+} \qquad \text{(A3)}$$

where $\nu_j = \nu_{ji} + \nu_{je}$, and $U_{nj} = (T_j/n_j e_j B)\,dn_j/dr$ is the diamagnetic velocity of the j^{th} species. Integrating f_{j+} over velocity gives an equation for n_{j+}.

$$\frac{n_{j+}}{n_o} = -\epsilon \frac{(v_o + U_{nj})}{2v_{tj}\Theta}\left[2z + \left(1 + 2z^2\right) Z(z)\right]\exp(i\theta)$$
$$+\left[\left(\frac{U_{nj}}{v_{tj}\Theta} - z\right) Z(z) - 1\right]\frac{e_j\phi_{1+}}{T_j} \qquad \text{(A4)}$$
$$-\frac{irv_j}{v_{tj}\Theta}\frac{n_{j+}}{n_o} - \frac{2ir}{v_{tj}^2\Theta}\left[1 + zZ(z)\right]\sum_k v_{jk}\, q_{k+}$$

where $z_j = x_j + iy_j = -v_o/v_{tj}\,\Theta + irv_j/v_{tj}\,\Theta$, and the subscript j is omitted from z_j in Eq (A4). The function Z(z) is defined in Eq. (6) and tabulated in Ref. [15, 16]. It is related to the function I(z) used in Ref. [13] by $I(z) = 1 + zZ(z)$. The parallel velocities q_{k+} may be eliminated using the continuity equation [13],
$\Theta q_{k+} = -v_o\,(n_{k+}/n_o) + U_{nk}\,(e_k\Phi_{1+}/T_k) - \epsilon\,(v_o + U_{nk})\exp(i\theta)$,
giving a relation between n_{j+} and Φ_{1+}.

Most neoclassical analyses neglect the poloidal variation in the electrostatic potential. $e\Phi_1/T = o(\epsilon\rho_{i\theta}/L_n)$, where L_n is the density scale length, and since $\rho_{i\theta}/L_n << 1$ is assumed, its effect was neglected compared with other $O(\epsilon)$ terms [21]. However, the $O(\epsilon)$ terms cancel, due to the high mobility of ions and electrons along the magnetic field, leaving residual terms of order $\epsilon\rho_{j\theta}/L_n$, i.e. comparable or less than the $\Phi_1(r, \theta)$ terms [22]. For example, in the standard neoclassical equilibrium $v_o + U_{ni} < U_{ni}$, and hence the first term in Eq. (A4) for the ions is less than $\epsilon\, U_{ni}/V_{ti}\Theta = \epsilon\rho_{i\theta}/L_n$. In the corresponding electron equation, the first term is of order $\epsilon\rho_{e\theta}/L_n$, and so the (usually neglected) second term is dominant. Hence Φ_{1+} should be retained. It is determined by the quasi-neutrality equation, $n_{i+} = n_{e+}$. Finally the mean particle flux is found by integrating the local flux over a magnetic surface

$$\Gamma_j = -\frac{1}{2\pi rB}\int_0^{2\pi} d\theta \int_{-\infty}^{\infty} dv_\parallel \int_0^{\infty} \pi dv_\perp^2 \left(f_{oj} + f_{1j}\right). \qquad \text{(A5)}$$
$$\left[\frac{\epsilon}{e_j} m_j \left(v_\parallel^2 + v_\perp^2/2\right)\sin\theta + \frac{\partial\Phi_1}{\partial\theta}\right][1 + \epsilon\cos\theta]^2$$

After rather lengthy analysis an expression of the following form was obtained for Γ_j [13].

$$\Gamma_j = \Gamma_j^{\alpha} + \Gamma_j^{\beta} + \Gamma_j^{\gamma} \tag{A6}$$

where

$$\Gamma_i^{\alpha} = \frac{\epsilon^2 n T_i}{2reB} \frac{(v_o + U_{ni})}{v_{ti}\Theta} \left\{ \mathrm{Im}\, Z(z) + \frac{\Lambda_i^I}{x\left(F^2 + L^2\right)} \cdot \right.$$

$$\left. \left(\left[g\left(1 + \frac{U_{ne}}{v_o}\right)\Lambda_e^R - \frac{U_{ne}}{v_o}(1+\tau) \right]^2 + \left[g\left(1 + \frac{U_{ne}}{v_o}\right)\Lambda_e^I \right]^2 \right) \right. , \tag{A7}$$

$$\Lambda_j = \Lambda_j^R + i\Lambda_j^I = \frac{1 + z_j\, Z_j}{1 + i y_j\, Z_j + 2i\, x_j\, y_j\, z_j\, Z_j}, \quad Z_j \equiv Z\left(z_j\right),$$

$$g = 1 + \tau + 2x_i^2 + 2\tau x_e^2, \qquad \tau = T_e / T_i$$

$$F + iL = \tau\,(1 + U_{ni}/v_o)\Lambda_i + (1 + U_{ne}/v_o)\Lambda_e.$$

Γ_i^{β} contains only terms proportional to ν_{ei}. In the strong collisional limit it goes into the Pfirsch-Schlüter flux for an arbitrary radial electric field. It is much less than Γ_i^{α} in conditions typical of H-mode edge plasmas. Γ_i^{γ} contains second order terms in the collision frequency, and is smaller than the other two except at very high collisionality.

In the collisionless limit the ImZ(z) term in Γ_i^{α} gives the plateau flux of Eqs. (1) and (4), as discussed in Sec. 2. As collisionality increases, this term takes the character of ion collisional viscosity, Im Z (z) ~ $y/(x^2 + y^2)$. In the calculations described in this paper, only the Im Z(z) term is retained. This function is well tabulated [15, 16] allowing rapid calculation over the parameter range of interest. The other terms in Eq. (A7) result from the inclusion of $\Phi_1(r, \theta)$, and from the

collisional terms included in Eq. (A1) to conserve particles and momentum. Some of them are of the same order as ImZ(z). They have the same asymptotic behaviour as ImZ(z) and thus may affect the magnitude of the ion current, by an 0(1) factor, but do not change the overall behavior nor the position of the maximum in Γ_i. Since the aim of this paper is to elucidate the underlying mechanism of the probe-triggered L-H transition and its parameter dependence, analytic detail is sacrificed for clarify.

APPENDIX B

EVOLUTION OF AN UNSTABLE POTENTIAL PROFILE

As discussed in Sec. 3, in a uniform plasma with a radially constant radial electric field, $E_r = V/s$, a space charge perturbation grows exponentially with time if $V > sE_m$, where E_m is the field at which the current maximum occurs. The evolution of a small positive space charge distribution $\rho(r, t)$, localised around some intermediate radius r = a-d, will now be considered. Values of parameters within the two ranges a-s <r < a-d-δ and a-d+d <r < a, where δ is the half-width of the charge distribution, will be denoted by subscripts 1 and 2 respectively.

The charge continuity equation, combined with Poisson's equation, gives

$$\frac{\partial \rho}{\partial t} = -\nabla \cdot j = -\frac{\partial j}{\partial E} \cdot \frac{\partial E}{\partial r} = -\frac{4\pi}{\epsilon_o} \frac{\partial j}{\partial E} \rho$$

Since $E > E_m$, $\partial j / \partial E < 0$ initially, and $\rho(r,t)$ grows exponentially. Because $\epsilon_o (E_2 - E_1) = 4\pi \int_{a-d-\delta}^{a-d+\delta} \rho \, dr$, E_1 must decrease and E_2 increase with time. Soon E_1 is pushed below E_m, as illustrated in Fig. B1(a). Over that part of the space charge where $E < E_m$, $\partial j/\partial E > 0$ locally, and so $\rho(r,t)$ locally decreases with time. This reduces the width of the space charge distribution. As a result of this local reduction in $\rho(r,t)$, the region where $E = E_1$ in Fig. B1(a) extends further to the right, thus increasing the radius where $E = E_m$. Thus the left-hand boundary of the space charge moves to larger r, causing the distribution to become narrower as it grows in height.

As E changes radially from E_1 to E_2, the local current, j(E), must follow the variation in Fig. 2, passing through a maximum where $E = E_m$. As discussed in Sec. 3, the instability continues until j_1 becomes equal to j_2, when the growth of the total space charge ceases. However, the space charge distribution may continue to narrow, and the transition from E_1 to E_2 becomes more abrupt, until the width becomes limited by ion Larmor radius effects. Trapped particle orbits do not impose a larger lower limit on the contraction, as they do in the plasma radial sheath [18]. This is because a particle ceases to be trapped when it crosses

the space charge layer. Trapped particles have $|v_{\|} - E_r/B_\theta| < \varepsilon^{1/2} V_{tj}$, and so, when there is a sudden large change in E_r, particles which are trapped on one side of the transition become passing particles on the other side. After the space charge width reaches its lower limit, the electric field profile is in a second equilibrium which, as shown in Appendix C, is stable.

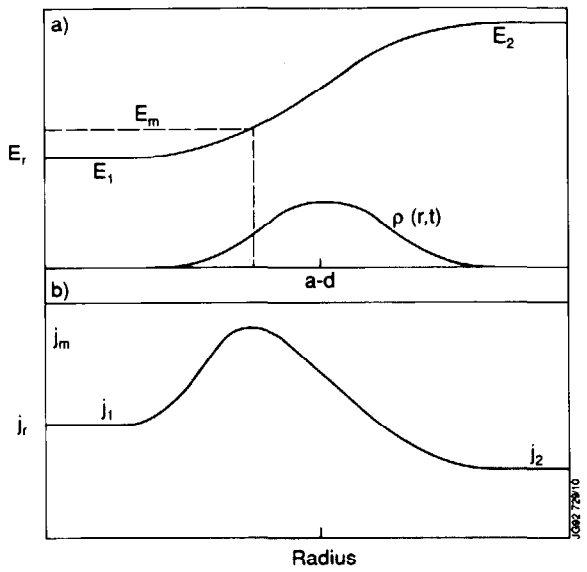

Fig. B1: Variation in (a) space charge and electric field and (b) current in the vicinity of r = a-d.

APPENDIX C

STABILITY OF THE DISCONTINUOUS ELECTRIC FIELD PROFILE

The stability of the bifurcated electric field profile in a uniform plasma, as illustrated by points A and B in Fig. 2, will now be studied. Such an equilibrium has a space charge $\sigma = \int \rho dr = \varepsilon_0 (E_2 - E_1)/4\pi$ localised close to a surface r = a-d. To simplify the argument, the small radial width of the space charge distribution will be neglected, and the jump in electric field treated as discontinuous.

Consider the effect of a small decrease in the surface charge σ. δE_1 and δE_2, the changes in E_1 and E_2 respectively, must satisfy δE_1 (s-d) + δE_2 d=0, with δE_1 positive and δE_2 negative. The currents across r = a-d are no longer equal, giving

$$\frac{d\sigma}{dt} = \delta j_1 - \delta j_2 = \left(\frac{\partial j}{\partial E}\right)_1 \delta E_1 - \left(\frac{\partial j}{\partial E}\right)_2 \delta E_2$$

$$= \left[\left(\frac{\partial j}{\partial E}\right)_1 d + \left(\frac{\partial j}{\partial E}\right)_2 (s-d)\right] \frac{\delta E_1}{d} \qquad \text{(C1)}$$

If $H \equiv [(\partial j/\partial E)_1 \, d + (\partial j/\partial E)_2 \, (s\text{-}d)]$ is positive, σ increases with time, returning the profile to its equilibrium. If H is negative, the space charge decreases and the field profile moves further away from equilibrium. The same stability criterion applies, of course, when the initial perturbation in surface charge is positive.

The effect of surface space charge on j_1 and j_2, the current flows on either side of the discontinuity is shown in Fig. C1. The jump in radial electric field,

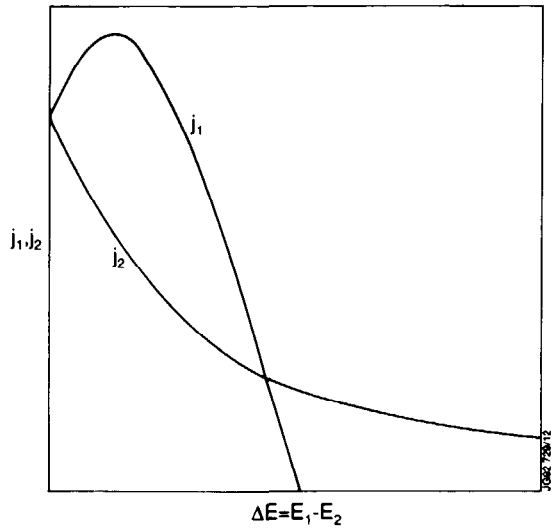

Fig. C1 *Variation in j_1 and j_2 with increasing surface space charge $\sigma = \varepsilon_0 \Delta E/4\pi$ at $r = a\text{-}d$, for $V > sE_m$.*

$\Delta E = E_2\text{-}E_1 = 4\pi\sigma/\varepsilon_0$. is chosen as the independent variable, rather than σ. Then $E_1 = [V\text{-}d\Delta E]/s$ and $E_2 = [V + (s\text{-}d)\,\Delta E]/s$, where V is the applied voltage. For each value of ΔE, $j_1 = j(E_1)$ and $j_2 = j(E_2)$ are given by the plasma current response, illustrated in Fig. 2. $\Delta E = 0$ corresponds to a continuous electric field equilibrium, where $j_1 = j_2 = j(V/s)$. When $V > s\,E_m$, j_2 decreases with increasing ΔE, while j, at first increases and then decreases rapidly. The second intersection of these two curves corresponds to the discontinuous equilibrium. At all other values of ΔE the profile is transient, since the current is not constant across $r = a\text{-}d$.

The difference in slopes between the j_1 (ΔE) and j_2 (ΔE) curves is

$$\frac{dj_1}{d(\Delta E)} - \frac{dj_2}{d(\Delta E)} = \left(\frac{dj_1}{dE_1}\right)\frac{dE_1}{d(\Delta E)} - \left(\frac{dj_2}{dE_2}\right)\frac{dE_2}{d(\Delta E)}$$

$$= -\frac{d}{s}\left(\frac{\partial j}{\partial E}\right)_{E_1} - \frac{s-d}{s}\left(\frac{\partial j}{\partial E}\right)_{E_2} = -\frac{H}{s} \qquad \text{(C2)}$$

Near the intersection at $\Delta E = 0$, the j_1 gradient is positive and the j_2 gradient is negative, so obviously $\partial j_1/\partial(\Delta E) - \partial j_2/\partial(\Delta E)$ is positive, i.e. H is negative confirming that a constant field profile is unstable. At the intersection

corresponding to the discontinuous equilibrium, both gradients are negative, but the j_1 gradient is steeper. Hence $\partial j_1/\partial(\Delta E) - \partial j_2/\partial(\Delta E)$ is negative, and the profile is stable. When $V < sE_m$, the shape of the j_1 and j_2 curves is interchanged. The continuous profile is then stable, and the discontinuous profile unstable.

We will now examine whether the discontinuous field profile is stable against the growth of a space charge perturbation localised at a different radius. Starting with a profile in which the radial field jumps from E_1 to E_2 at r = a-d, we first introduce a small positive surface charge at some radius r = a-f, where f < d. This surface charge gives rise to a small jump in E_r at r = a-f. The values of parameters within the radial range a-s < r < a-d (the original region 1) will now be denoted by subscript 3, those in a-d < r < a-f by subscript 4, and in a-f < r < a by subscript 5. The total potential is unchanged, i.e.

$$(s-d)(E_3-E_1) + (d-f)(E_4-E_2) + f(E_5 - E_2) = 0 \qquad (C3)$$

Since the surface charge already at r = a-d is not changed initially, immediately after the perturbation $E_4 - E_3 = E_2 - E_1$. If we write $E_3 = E_1 - \Delta E$ (so ΔE is positive), then $E_4 = E_2 - \Delta E$ and $E_5 = E_2 + \Delta E\,(s-f)/f$.

Now consider whether the perturbation charge at r = a-f initially grows or decays. This depends on the sign of

$$j_4 - j_5 = j_2 - \left(\frac{\partial j}{\partial E}\right)_2 \Delta E - j_2 - \left(\frac{\partial j}{\partial E}\right)_2 \frac{(s-f)}{f}\Delta E = -\left(\frac{\partial j}{\partial E}\right)_2 \frac{s}{f}\Delta E \qquad (C4)$$

where $(\partial j/\partial E)_2$ is the gradient of the j vs. E curve at $E = E_2$. Since E_2 is on the decreasing section of the curve, $j_4 - j_5$ is positive, and so the surface charge at r = a-f grows with time. Next consider whether the finite surface charge already at r = a-d increases or decreases. This depends on

$$j_3 - j_4 = \left[-\left(\frac{\partial j}{\partial E}\right)_1 + \left(\frac{\partial j}{\partial E}\right)_2\right]\Delta E$$

Since $(\partial j/\partial E)_1$ is positive, and $(\partial j/\partial E)_2$ is negative, $j_3 - j_4$ is negative and so the original surface charge at r = a-d decreases.

Applying the same reasoning when $f > d$, i.e. when the charge perturbation is located between the probe and the field discontinuity, shows that such a perturbation decays with time. Thus a discontinuous equilibrium electric field is unstable to the growth of a surface charge at any larger radius, but not at smaller radii. Extrapolation of the initial behaviour leads one to expect that the initial surface charge at $r = a-d$ decays, to be replaced by a surface charge and field discontinuity at $r = a-f$. A strict application of this conclusion implies that when $V > sE_m$ the only completely stable field profile is one with a discontinuity at $r = a$. The corresponding equilibrium has very low current, with most of the voltage drop occurring over a vanishing narrow edge layer where the electric field is very large. In practice the foregoing argument is likely to become invalid within some distance b from the boundary due, for example, to impurities and neutrals or to the orbit loss current. The only stable profile then has a field discontinuity at $r = a-b$.